Extremophiles (2004) 8:507–512
DOI 10.1007/s00792-004-0411-6

ORIGINAL PAPER

Thomas Hansen · Claus Urbanke · Peter Schönheit

Bifunctional phosphoglucose/phosphomannose isomerase from the hyperthermophilic archaeon *Pyrobaculum aerophilum*

Received: 23 March 2004 / Accepted: 14 June 2004 / Published online: 3 August 2004

Abstract ORF PAE1610 from the hyperthermophilic crenarchaeon *Pyrobaculum aerophilum* was first annotated as the conjectural *pgi* gene coding for hypothetical phosphoglucose isomerase (PGI). However, we have recently identified this ORF as the putative *pgi*/*pmi* gene coding for hypothetical bifunctional phosphoglucose/phosphomannose isomerase (PGI/PMI). To prove its coding function, ORF PAE1610 was overexpressed in *Escherichia coli*, and the recombinant enzyme was characterized. The 65-kDa homodimeric protein catalyzed the isomerization of both glucose-6-phosphate and mannose-6-phosphate to fructose-6-phosphate at similar catalytic rates, thus characterizing the enzyme as bifunctional PGI/PMI. The enzyme was extremely thermoactive; it had a temperature optimum for catalytic activity of about 100°C and a melting temperature for thermal unfolding above 100°C.

Keywords Hyperthermophilic archaea · Phosphoglucose/phosphomannose isomerase · *Pyrobaculum aerophilum*

Introduction

Phosphoglucose isomerase (PGI; EC 5.3.1.9) catalyzes the reversible isomerization of glucose-6-phosphate (G6P) to fructose-6-phosphate (F6P). PGI plays a central role in sugar metabolism of eukarya, bacteria, and archaea, both in glycolysis via the Embden-Meyerhof pathway in eukarya and bacteria and in its modified versions found in archaea. PGI is also involved in gluconeogenesis, where the enzyme operates in the reverse direction (for literature, see Hansen et al. 2001; Noltmann 1972; Schönheit and Schäfer 1995).

PGIs evolved convergently and belong either to the PGI superfamily or to the cupin superfamily. Cupin-type PGIs were found in some euryarchaea (Hansen et al. 2001; Jeong et al. 2003; T. Hansen, unpublished data). Recent identification of bifunctional phosphoglucose/phosphomannose isomerase (PGI/PMI) divided the PGI superfamily into the PGI family and the PGI/PMI family (Hansen et al. 2004). Whereas a variety of PGIs from the domains of eukarya and bacteria as well as euryarchaeon *Methanococcus jannaschii* (Rudolph et al. 2003) are well studied, only the PGI/PMIs from the archaea *Aeropyrum pernix* (ApPGI/PMI) and *Thermoplasma acidophilum* (TaPGI/PMI) have been characterized so far. Both PGI/PMIs catalyzed the isomerization of both G6P and mannose 6-phosphate (M6P) at equal catalytic rates and thus combine both the function of a PGI and a PMI. Sequence comparison revealed several putative homologues in two (hyper)thermophilic bacteria and several archaea including *Pyrobaculum aerophilum* (ORF PAE1610). To prove the coding function of ORF PAE1610, which was previously annotated as the conjectural *pgi* gene (Fitz-Gibbon et al. 2002), it was functionally overexpressed in *Escherichia coli*. The recombinant enzyme catalyzed the isomerization of both G6P and M6P at similar rates, defining the enzyme as a bifunctional PGI/PMI—PaPGI/PMI. Thus, ORF PAE1610 represents the *pgi*/*pmi* gene coding for the third characterized member of the novel bifunctional PGI/PMI family. Since PaPGI/PMI is overexpressed in *E. coli* at high levels, the enzyme is an ideal candidate for crystallization and elucidation of the 3-D structure to analyze the structural basis for the bifunctionality of this novel protein family.

Communicated by G. Antranikian

T. Hansen · P. Schönheit (✉)
Institut für Allgemeine Mikrobiologie,
Christian-Albrechts-Universität Kiel,
Am Botanischen Garten 1-9,
24118 Kiel, Germany
E-mail: peter.schoenheit@ifam.uni-kiel.de
Tel.: +49-431-8804328
Fax: +49-431-8802194

C. Urbanke
Institut für Biophysikalisch-Biochemische Verfahren
Medizinische Hochschule, Carl Neuberg Str. 1,
30625 Hannover, Germany

Materials and methods

Cloning, overexpression, and purification of PGI/PMI from *Pyrobaculum aerophilum*

The coding region of ORF PAE1610 was amplified from *Pyrobaculum aerophilum* genomic DNA by PCR with *Pwo* polymerase (PEQLAB, Germany). The following primers were used to introduce unique restriction sites for *Nde*I and *Xho*I, respectively: CCATTGCTAGTGAGAAA CATATGAGCCAA (forward) and GCCTTCTACG CTCGAGATACAGTAGTCAC (reverse). Following *Nde*I/*Xho*I double digestion, the PCR product was inserted by T4 DNA ligase (Roche Diagnostics) into pET17b expression vectors (Novagen) linearized by *Nde*I/*Xho*I double digestion. The resulting plasmid pET17b-*papgipmi* was introduced into *Escherichia coli* JM109 and BL21-CodonPlus(DE3)-RIL (Stratagene) via transformation. The transformed cells were grown at 37°C in two flasks, each containing 400 ml Luria-Bertani medium with 100 μg/ml carbenicillin and 34 μg/ml chloramphenicol. When the cells reached an optical density at 600 nm of 0.8, protein expression was induced by the addition of 0.4 mM IPTG. After a further 4 h of growth (OD_{600}, ~2.5–3.2), the cells were harvested by centrifugation at 4°C and then washed in a buffer containing 50 mM Tris-HCl (pH 7.0) and 50 mM NaCl. Cell extracts were prepared by French press treatment (1.3×10^8 Pa) of cell suspensions in buffer A (50 mM sodium phosphate). After ultracentrifugation (100,000 *g* for 60 min), the solution was heat-precipitated at 90°C for 45 min, centrifuged again (15,000 *g* for 30 min), extensively dialyzed against buffer B [2 M ammonium sulfate 50 mM Tris-HCl (pH 8.0)], and applied to a phenyl Sepharose column (15 ml) previously equilibrated with buffer B. Protein was eluted by a linear ammonium sulfate gradient (2–0 M, 90 ml), followed by washing the column with 30 ml 50 mM Tris-HCl (pH 8.0). Fractions containing PaPGI/PMI activity (33 ml, 0.32–0 M ammonium sulfate) were checked for purity with respect to protein and DNA impurities. Only almost-pure PaPGI/PMI (15 ml, 0.14–0 M ammonium sulfate) was used for further purification, concentrated by ultrafiltration (exclusion size, 10 kDa) and then applied to a Superdex 200 gel filtration column (120 ml) equilibrated with buffer C [(150 mM NaCl, 50 mM Tris-HCl (pH 7.5)]. From this step, pure PaPGI/PMI was obtained (77–94 ml). Finally, the purified protein was dialyzed against 10 mM Tris-HCl pH 8.0 and concentrated to 30 mg/ml using ultrafiltration.

Analytical assays

The purity of the preparation was checked by SDS-PAGE in 12% gels, followed by staining with Coomassie Brilliant Blue R 250, according to standard procedures (Laemmli 1970). The protein concentration of purified recombinant protein was determined using the molar extinction coefficients at 280 nm of the enzymes as calculated by the ProtParam [http://us.expasy.org/tools/protparam.html]: PaPGI/PMI = 36,840 M cm^{-1}. Molecular mass determinations were performed by analytical ultracentrifugation in a Beckman Optima XL-A analytical ultracentrifuge equipped with a Titan AN 50 rotor and absorption optics as recently described for TaPGI/PMI (Hansen et al. 2004). Circular dichroism (CD) spectroscopy analysis and temperature-gradient experiments to follow heat-induced unfolding of PaPGI/PMI were performed on a JASCO J-715 CD spectrometer as previously described (Hansen et al. 2004). Secondary structure analysis and assignments to different secondary structure types were performed by the experimentally established spectra–structure correlation, using the varselec option of Dicroprot (Deleage and Geourjon 1993). The program PredictProtein was used for sequence based secondary structure predictions [http://cubic.bioc.columbia.edu].

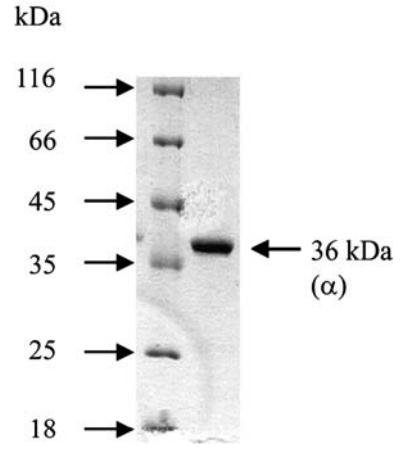

Fig. 1 Purified recombinant *Pyrobaculum aerophilum* bifunctional phosphoglucose/phosphomannose isomerase (PaPGI/PMI) as analyzed by SDS-PAGE. Protein was denatured in a 12% polyacrylamide slab gel (8×7 cm), which was stained with Coomassie Brilliant Blue R-250. *Lane 1* Molecular mass standard, *lane 2* 1.5 μg purified recombinant PaPGI/PMI

Enzyme assays and determination of kinetic parameters

Kinetic parameters were measured for both PGI and PMI activity. PGI activity (G6P↔F6P) was determined in both directions and PMI (M6P↔F6P) activity in the direction of F6P formation at pH 7.4 (optimal pH). The formation of G6P and F6P was measured using G6P dehydrogenase from *Thermotoga maritima* (Hansen et al. 2002) and mannitol-1-phosphate dehydrogenase from *Klebsiella pneumoniae* (Otte and Lengeler 2001) or *Pyrococcus furiosus* PGI (PfcPGI) (Hansen et al. 2001) as previously described for ApPGI/PMI (Hansen et al. 2004). In standard assays 2 μg enzyme was used. Erythrose-4-phosphate and 6-phosphogluconate were tested for potential inhibitory effect on PaPGI/PMI. The temperature dependence of enzyme activity was

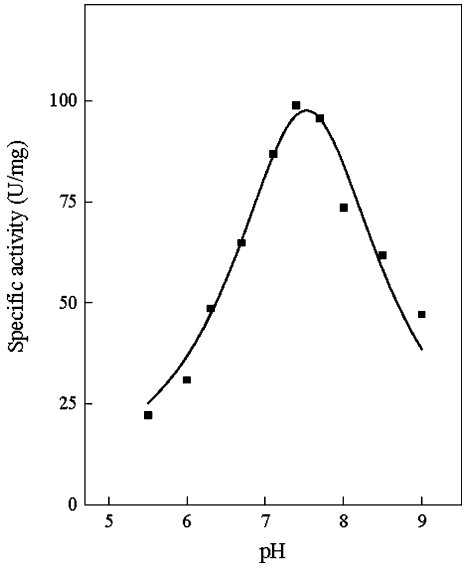

Fig. 2 Effect of pH on the specific activity of PaPGI/PMI at 80°C

measured between 20 and 110°C in 50 mM sodium phosphate with F6P as substrate (5 mM), using either a continuous assay (below 100°C) or a discontinuous assay (above 100°C) as previously described (Hansen et al. 2001).

The thermostability of the purified enzyme (2 μg enzyme, pH 7.0) was tested in sealed vials that were incubated at temperatures between 90 and 110°C for 2–120 min. The vials were then cooled on ice for 10 min, and residual enzyme activity was tested and compared to the controls (unheated samples).

Sequence handling

Protein sequences were extracted from the NCBI, GenBank, and Pfam databases. Sequence alignments were constructed with the neighbor-joining (NJ) method of Clustal X, using the GONNET matrix (Thompson et al. 1997). Phylogenetic trees were constructed using the NJ option of Clustal X, and the maximum-likelihood (ML) method in PROML (PHYLIP, version 3.6) Confidence limits were estimated by 100 bootstrapping replicates.

Table 1 Molecular and kinetic properties of *Pyrobaculum aerophilum* bifunctional phosphoglucose/phosphomannose isomerase. The molecular mass of native enzyme was determined by analytical ultracentrifugation, that of subunits by SDS-PAGE

Parameter	Value
Arrhenius activation energy (23–89°C) (kJ/mol)	40.1
T_m (°C)	100 ± 3
$t_{1/2}$ (100°C) (min)	60
K_m (mM)	
F6P	
(50°C)	0.30 ± 0.06
(80°C)	0.06 ± 0.01
G6P	
(50°C)	2.7 ± 0.4
(80°C)	1.9 ± 0.4
M6P	
(80°C)	0.49 ± 0.08
V_{max} (U/mg)	
F6P	
(50°C)	31.3 ± 2.2
(80°C)	109 ± 5.5
G6P	
(50°C)	50 ± 3
(80°C)	150 ± 12
M6P	
(80°C)	117 ± 7
K_i (μM)	
Erythrose-4-phosphate	1.4 ± 0.2
6-Phosphogluconate	110 ± 10

Results and discussion

Expression of *papgi/pmi* and purification of the recombinant enzyme

ORF PAE1610 has been previously annotated as conjectural PGI. The ORF contains 909 bp coding for a

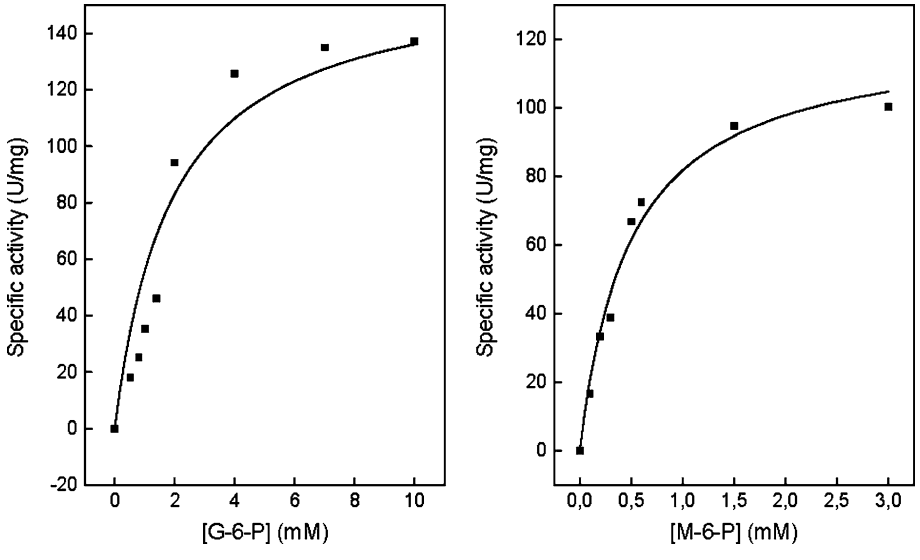

Fig. 3 Rate dependence of bifunctional PaPGI/PMI on glucose-6-phosphate (*left*) and mannose-6-phosphate concentration (*right*)

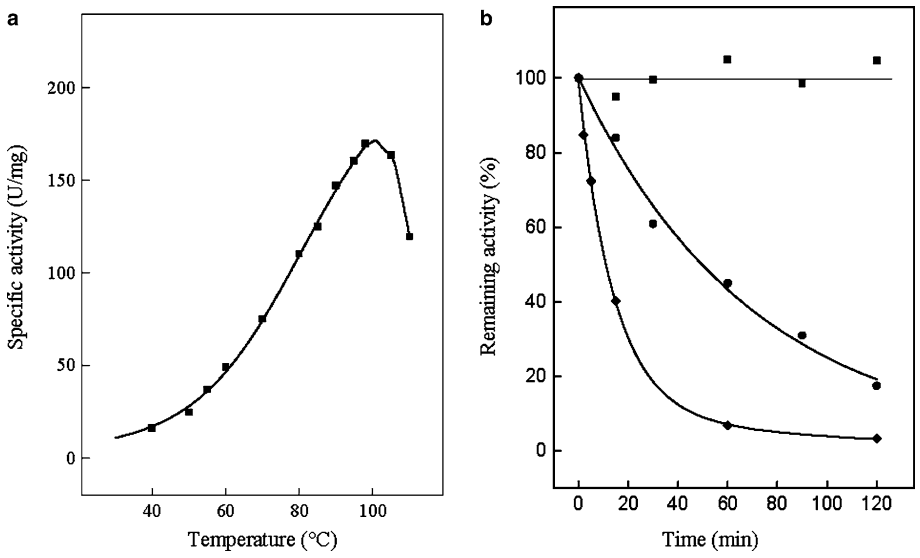

Fig. 4a, b Effect of temperature on the specific activity and thermostability of PaPGI/PMI. **a** PaPGI/PMI temperature dependence, **b** PaPGI/PMI thermostability at 90°C (*filled squares*), 100°C (*filled circles*), and 110°C (*filled diamonds*)

polypeptide of 302 amino acids with a calculated molecular mass of 33.548 kDa. To prove its coding function, PAE1610 was overexpressed in *Escherichia coli*. PaPGI/PMI was found in both the cytosolic fraction and to a significant extent, in inclusion bodies. The recombinant enzyme was purified from the cytosolic fraction about 80-fold from *E. coli* transformants by three steps. After the fist step, a 45-min heat treatment at 90°C, the PaPGI/PMI showed a specific activity of about 97 U/mg (80°C, F6P) and was apparently almost pure (>95%) with respect to protein content. About 20–30% of PaPGI/PMI was lost in this step due to coprecipitation with *E. coli* proteins. The following purification step on phenyl Sepharose was used to remove both residual contaminating protein and to a major extent, DNA impurities, which might influence crystallization of the enzyme. At this stage, PaPGI/PMI showed a specific activity of about 103 U/mg. However, about 40% of the PaPGI/PMI from this step was not used for further purification due to DNA content greater than 4%. Gel filtration chromatography was used as the final step. An additional 15% of the protein was lost by this step, but ultrapure PaPGI/PMI (>99.5%) was obtained that showed a specific activity of 103–109 U/mg. The purified enzyme catalyzed the isomerization of both G6P and M6P at similar catalytic efficiency, characterizing the protein as bifunctional PGI/PMI. The expression rate of PaPGI/PMMI was about five times higher as compared to ApPGI/PMI, which mainly forms inclusion bodies (Hansen et al. 2004). Thus, heterologous expression of PAPGI/PMI instead of ApPGI/PMI allows the production of PGI/PMI in large quantities (about 2 mg pure protein was obtained from 1 g transformed *E. coli*), a prerequisite for further biophysical and crystallographic studies.

Molecular properties

Purified recombinant PaPGI/PMI showed an apparent molecular mass of 65 kDa when analyzed by sedimentation–diffusion equilibrium runs performed by analytical ultracentrifugation. The calculated molecular mass of the PaPGI/PMI subunit was 33.548 kDa, and apparent molecular mass of the subunit as analyzed by SDS-PAGE was 36 kDa (Fig. 1), suggesting a homodimeric structure. The homodimeric structure was verified by analytical ultracentrifugation, which revealed a native molecular mass of 65 ± 4 kDa. Secondary structure analysis of the PaPGI/PMI was performed by CD spectroscopy. The recorded CD spectrum (not shown) was about superimposable when compared to the corresponding CD spectra of *Aeropyrum pernix* and *Thermoplasma acidophilum* (Hansen et al. 2004), indicating a very similar fold of the three PGI/PMIs. From the CD spectrum, an α-helical content of 40% and a β-sheet content of 17% were estimated, which about matches the secondary structure predictions (50% α helical and 14% β sheet).

Catalytic properties

The PaPGI/PMI showed a pH optimum at 7.4 (Fig. 2). About 50% of activity was found at pH 6.3 and 8.8, respectively. Kinetic properties of bifunctional PGI/PMI were analyzed for both reaction directions of PGI activity and in the direction of F6P formation of PMI activity (Fig. 3a, b; Table 1). Catalytic efficiencies with G6P and M6P were comparable, indicating that both catalytic functions might be used in vivo. Accordingly, genes encoding for a conventional PGI or a cupin-type PMI were not annotated and could not be identified in the completely sequenced genome of *Pyrobaculum aerophilum* (Fitz-Gibbon et al. 2002). The enzyme was inhibited by low concentrations of 6-phosphogluconate and especially erythrose-4-phosphate, which is a common property of enzymes of the PGI superfamily (see Rudolph et al. 2003).

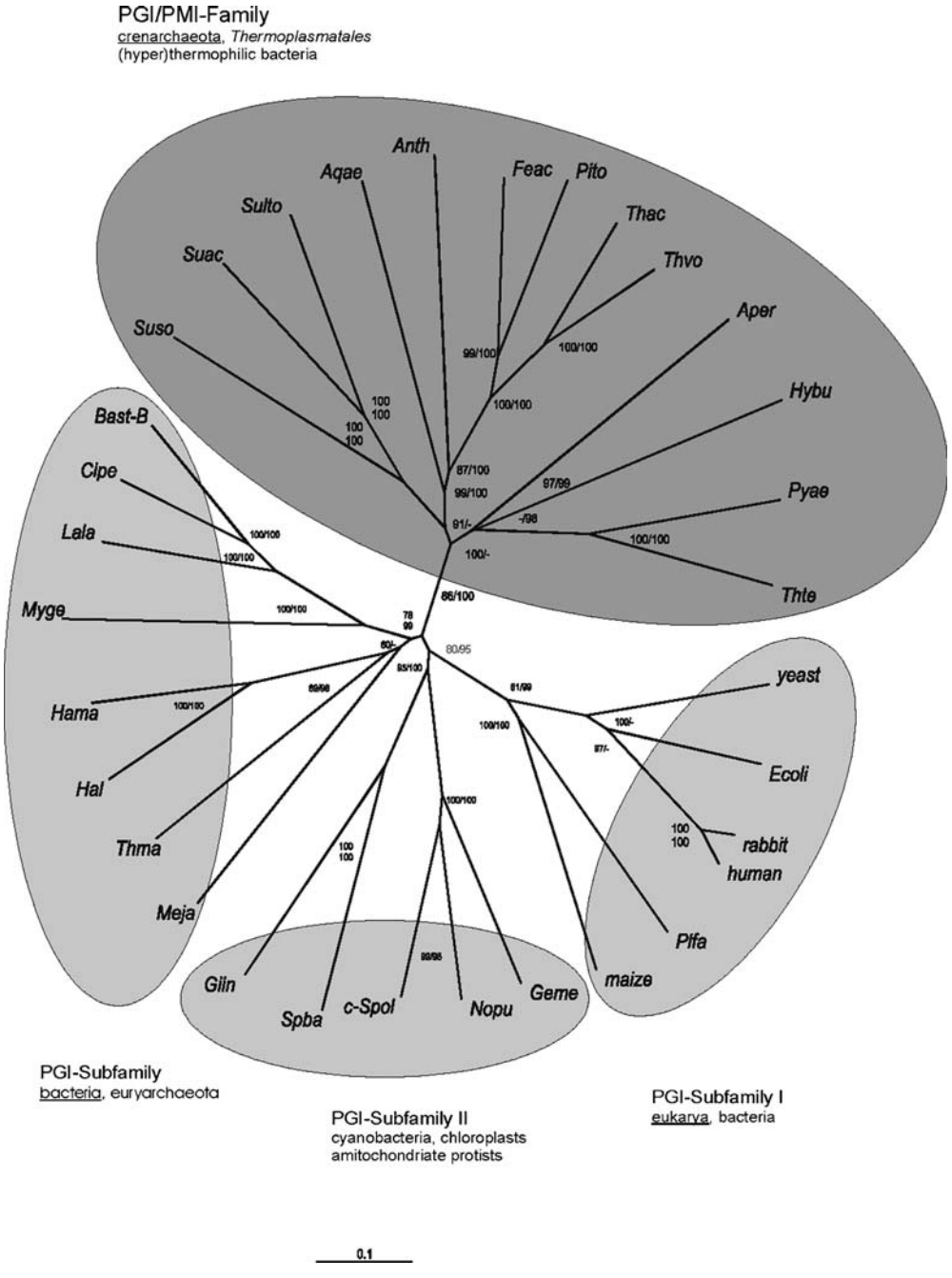

Fig. 5 Phylogenetic relationship of enzymes from the phosphoglucose isomerase (PGI) superfamily as constructed by the neighbor-joining (NJ) method of Clustal X (Thompson et al. 1997). The *numbers at the nodes* are bootstrapping values according to the NJ method (*first number*) and maximum-likelihood method (*second number*). Only values greater than 60 are given. NCBI accession numbers or SwissProt identifiers: *Aper*, *Aeropyrum pernix* BAA79746; *Pyae*, *P. aerophilum* AAL63599; *Thte*, *Thermoproteus tenax* CAF18453; *Suso*, *Sulfolobus solfataricus* NP_343653; *Sulto*, *Sulfolobus tokodaii* NP_378246; *Thvo*, *Thermoplasma volcanium* NP_111957; *Thac*, *Thermoplasma acidophilum* AL445067; *Feac*, *Ferroplasma acidarmanus* ZP_00001609; *Anth*, *Anaerocellum thermophilum* CAA93628; *Aqae*, *Aquifex aeolicus* NP_213515; *Meja*, *Methanococcus jannaschii* Q59000; *Thma*, *Thermotoga maritima* Q9X1A5; *Hal*, *Halobacterium* NRC1 Q9HNQ6; *Hama*, *Haloarcula marismortui* (retrieved from http://zdan2.umbi.umd.edu); *Lala*, *Lactococcus lactis* P81181; *Clpe*, *Clostridium perfringens* Q8XI54 *Bast-B*, *Bacillus stearothermophilus* B P13376; *Ecoli*, *Escherichia coli* P11537; *human*, P06744; *pig*, P08059; *rabbit*, Q9 N1E2; *yeast*, P12709; *maize*, *Zea mays* P49105; *Geme*, *Geobacter metallireducens* 23053592; *Nopu*, *Nostoc punctiforme* 23125809; *c-Spol*, *Spinacia oleracea* chloroplast T09153; *Spba*, *Spironucleus barkhanus* AAL56572; *Giin*, *Giardia intestinalis* AAK49040. Unpublished: *Thte*, *T. tenax*; *Hybu*, *Hyperthermus butylicus*; *Suac*, *Sulfolobus acidocaldarius*; *Pito*, *Picrophilus torridus*

Thermophilic properties

PaPGI/PMI exhibited extreme thermophilic properties. It showed a temperature optimum at about 100°C (Fig. 4a) and declined at temperatures above 105°C; about 70% of optimal activity was found at 110°C. Unfolding of the enzyme as monitored by CD spectroscopy at 221 nm could not be detected up to 100°C. At 100°C the half-life of PAPGI/PMI was about 60 min and at 110°C, about 10 min. Along with ApPGI/PMI and PfcPGI (Hansen et al. 2001, 2004), which had longer half-lives at 100°C, PaPGI/PMI represents the most thermostable and thermoactive PGI described so far, whereas PMIs from thermophiles have not been characterized yet. These thermophilic properties are in accordance with the optimal growth temperature of *P. aerophilum* (100°C, Völkl et al. 1993).

Sequence comparison and phylogenetic implications

Functional characterization clearly groups PaPGI/PMI into the PGI/PMI family within the PGI superfamily (Hansen et al. 2004). PaPGI/PMI shows 36% similarity

to ApPGI/PMI compared with 14–21% to members of the PGI-family. Additional putative PGI/PMIs had been identified in two *Sulfolobales* species, in three *Thermoplasmatales* species, and in two bacterial species. Due to the distribution of PGI/PMIs and phylogenetic analyses performed, a crenarchaeal origin of the PGI/PMI family was proposed, which could not be ambiguously resolved (Hansen et al. 2004). For clarification, additional phylogenetic analyses were performed, which included four additional PGI/PMI homologues: one from the crenarchaeon *Thermoproteus tenax*, the yet unpublished homologues from the crenarchaeota *Hyperthermus butylicus* and *Sulfolobus acidocaldarius*, and from the euryarchaeon *Picrophilus torridus*. Indeed, these four archaeal sequences were grouped into the PGI/PMI-family (Fig. 5). The overall topology of the tree shown was achieved by the methods used and is supported by good bootstrapping values. However, additional clarification of the origin of the PGI/PMI family could not be achieved by the tree reconstruction methods used. The NJ and the ML analyses still differ with respect to the basal nodes of the bacterial as well as the *Thermoplasmatales* sequences. According to the NJ analysis, the two bacterial sequences as well as the four *Thermoplasmatales* sequences still cluster close to the *Sulfolobales* sequences, which is in accordance with a crenarchaeal origin and would imply an early gene transfer from an ancestral *Sulfolobus* species as recently suggested (Hansen et al. 2004). Although the presence of PGI/PMIs in euryarchaeota remains restricted to *Thermoplasmatales* species, the ML analysis still revealed two PGI/PMI groups, a crenarchaeal group and a *Thermoplasmatales* group, suggesting an archaeal origin of this family. Thus, this question remains open until significantly more archaeal PGI/PMI sequences will be available.

Acknowledgements We thank B. Siebers, H.P. Klenk, W. Liebl, and P. Redder for providing us—prior to publication—the PGI/PMI sequences from *T. tenax*, *H. butylicus*, *P. torridus*, and *S. acidocaldarius*, respectively. The expert technical assistance of A. Brandenburger and K. Lutter-Mohr is gratefully acknowledged. Some preliminary experiments on cloning and expression of PaPGI/PMI were performed by D. Knierim in an advanced student course. This work was supported by grants of the Deutsche Forschungsgemeinschaft (SCHO 316/9-1) and the Fonds der Chemischen Industrie.

References

Deleage G, Geourjon C (1993) An interactive graphic program for calculating the secondary structure content of proteins from circular dichroism spectrum. Comput Appl Biosci 9:197–199

Fitz-Gibbon ST, Ladner H, Kim UJ, Stetter KO, Simon MI, Miller JH (2002) Genome sequence of the hyperthermophilic crenarchaeon *Pyrobaculum aerophilum*. Proc Natl Acad Sci USA 99:984–989

Hansen T, Oehlmann M, Schönheit P (2001) Novel type of glucose-6-phosphate isomerase in the hyperthermophilic archaeon *Pyrococcus furiosus*. J Bacteriol 183:3428–3435

Hansen T, Schlichting B, Schönheit P (2002) Glucose-6-phosphate dehydrogenase from the hyperthermophilic bacterium *Thermotoga maritima*: expression of the *g6pd* gene and characterization of an extremely thermophilic enzyme. FEMS Microbiol Lett 216:249–253

Hansen T, Wendorff D, Schonheit P (2004) Bifunctional phosphoglucose/phosphomannose isomerases from the archaea *Aeropyrum pernix* and *Thermoplasma acidophilum* constitute a novel enzyme family within the phosphoglucose isomerase superfamily. J Biol Chem 279:2262–2272

Jeong JJ, Fushinobu S, Ito S, Jeon BS, Shoun H, Wakagi T (2003) Characterization of the cupin-type phosphoglucose isomerase from the hyperthermophilic archaeon *Thermococcus litoralis*. FEBS Lett 535:200–204

Laemmli UK (1970) Cleavage of structural proteins during the assembly of the head of bacteriophage T4. Nature 227:680–685

Noltmann EA (1972) Aldose-ketose isomerases. In: Boyer PD (ed) The enzymes, 3rd edn. Academic, New York, pp 271–354

Otte S, Lengeler JW (2001) The *mtl* genes and the mannitol-1-phosphate dehydrogenase from *Klebsiella pneumoniae* KAY2026. FEMS Microbiol Lett 194:221–227

Rudolph B, Hansen T, Schönheit P (2003) Glucose-6-phosphate isomerase from the hyperthermophilic archaeon *Methanococcus jannaschii*, characterization of the first archaeal member of the phosphoglucose isomerase superfamily. Arch Microbiol 181:82–87. DOI 10.1007/s00203-003-0626-4

Schönheit P, Schäfer T (1995) Metabolism of hyperthermophiles. World J Microbiol Biotechnol 11:26–57

Thompson JD, Gibson TJ, Plewniak F, Jeanmougin F, Higgins DG (1997) The CLUSTAL_X windows interface: flexible strategies for multiple sequence alignment aided by quality analysis tools. Nucleic Acids Res 25:4876–4882

Völkl P et al (1993) *Pyrobaculum aerophilum* sp. nov., a novel nitrate-reducing hyperthermophilic archaeum. Appl Environ Microbiol 59:2918–2926